European Drag Reduction and Flow Control Meeting – EDRFCM 2015
March 23–26, 2015, Cambridge, UK

INTERACTION OF FLEXIBLE FILAMENTS WITH THE WAKE OF CYLINDER AT LOW REYNOLDS NUMBERS

M. Omidyeganeh and A. Pinelli
Department of Mechanical and Aeronautical Engineering, City University London, EC1V 0HB, London, UK

INTRODUCTION

Flows over bluff bodies are encountered in a variety of engineering applications and have commonly been one of the fundamental topics in fluid mechanics. One of the paradigmatic examples is the flow behind a circular cylinder and its control, which has been studied extensively in experiments, theoretical models, and numerical simulations. In particular, the transition of two-dimensional vortex shedding from either side of the cylinder at low Reynolds numbers ($Re_D = U_\infty D/\nu < 180$, where D is the diameter of cylinder, and U_∞ is the upstream velocity) to a three-dimensional wake characterised by irregular vortices at higher Reynolds numbers ($Re_D > 270$) has been investigated for more than half a century.

It is well known that the three dimensional transition of the cylinder near-wake is characterised by two fundamental unstable modes. The first three-dimensional unstable mode (mode A) is induced by an elliptic instability in the near-wake vortex cores. Mode A instability attenuates as Re_D is further increased over the critical value of $\simeq 180$. The spanwise wavelength of mode A is between 3 to 4 diameters [4]. At larger Reynolds numbers, an intermittent behaviour between 2D laminar rollers and 3D streamwise undulations superimposed on the rollers is observed. For values of $Re_D > 270$, a second (mode B) instability appears. The latter is associated with a region of hyperbolic flow in the braided shear layer. The spanwise wavelength of B mode is approximately equal to the cylinder diameter.

The main objective of the present work is to introduce a passive control technique to interfere with the three dimensional transition of the wake. In particular, as control elements we will introduce a set of flexible filaments on the lee side of the cylinder. To preserve the symmetry of the geometry and to simplify the analysis we have considered a uniform spanwise distribution of filaments along the symmetry line of the mean flow. Thus, filaments flexibility, length and spacing are the parameters that will determine the coupled interaction between the fluid flow and the flexible elements. In particular, the flapping of the filaments, caused by their interaction with the vorticity field, will be modified by modifying the flexibility. To interfere with the 3D instability mechanisms at different Reynolds numbers, the spacing between the filaments will be tuned according to the wavelength of the dominant modes.

PROBLEM FORMULATION

Figure 1 shows a scheme of the geometry under consideration (a fixed infinite cylinder with a number of filaments uniformly distributed on the lee side) and the definition of the Cartesian reference system (u, v and w will be used to indicate the streamwise, vertical and spanwise components of the flow velocity field). The filaments are attached to the lee side of the cylinder and clamped with a specified normal vector n_f. In all cases n_f is aligned with x if not differently stated. The flow field is numerically integrated by discretising in space and time the three dimensional, unsteady Navier-Stokes equations. In particular, a second order accurate centred finite volume method is used for the space discretisation, while the time advancement is carried out via a semi-implicit (Crank-Nicolson scheme for the vertical diffusive terms, and the Adams-Bashforth scheme for all the others) fractional-step method. The resulting code is parallelised using the Message-Passing Interface exploiting the domain-decomposition technique. The code has been extensively tested and validated in the past (see [2] for a detailed description). The presence of the cylinder and the filaments are modelled by introducing a system of body forces in the momentum equations. The cylinder surface fixed boundary is handled by using a bi-linear direct-forcing immersed-boundary method. The moving boundaries determined by the presence of the filaments are tackled using the RKPM method [3]. The latter methodology also provide for the hydrodynamic force exerted by the fluid on the filaments at each time step.

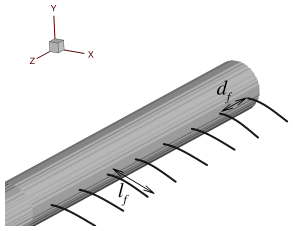

Figure 1: Schematic of the cylinder with attached filaments.

The filament motion is modelled by Timosheko beam theory [1]:

$$\Delta\rho \frac{\partial^2 x_i}{\partial t^2} = \frac{\partial}{\partial s}\left(T\frac{\partial x_i}{\partial s}\right) - K_B \frac{\partial^4 x_i}{\partial s^4} - \rho_f a_f \epsilon, \qquad (1)$$

where $x_i, i = 1 \cdots 3$ are the Cartesian displacements (in x, y and z), s is the filament parametric coordinate, T is the tension of filament, K_B is the stiffness of filament, ρ_f is density of fluid, a_f is acceleration of fluid at the position of filament (related to the force imposed on the fluid computed by immersed boundary method), ϵ is the characteristics hydraulic cross section area of the filament (here is approximately equal to the mesh cell face). $\Delta\rho = \hat{\rho}_s - \hat{\rho}_f$ is the difference in density per unit area of filament cross section between solid filament and fluid. The filament dynamic equation (1) is advanced in time (under the constraint of inextensibility: $(x_i\ x_i)^{1/2} = 1$)

by solving the algebraic non-linear system, arising after a finite difference approximation, via a Newton Raphson method at each time step [1].

A series of direct numerical simulations were carried out at $Re = 100$, 200, and 300 with and without filaments. The size of the domain is $21D$, $10D$, and $8D$ in the streamwise, vertical, and spanwise directions respectively. Simulations without filaments are validated against experiments by comparing the drag and lift forces on the cylinder as well as characteristics of the structures. Grid refinement studies were carried out for these simulations to ensure independence of the statistics and instantaneous structures at the current grid resolution. The number of Eulerian grid points is $482 \times 274 \times 96$ while 38 Lagrangian points are used for each filament representation.

RESULTS AND DISCUSSIONS

Figure 2 illustrates coherent flow structures in the wake of an unmodified cylinder at three different Reynolds numbers: $Re_D = 100$ is characterised by a 2D wake; at $Re_D = 200$ the 2D rollers are undulated in the span by an unstable mode (A wavelength $\simeq 4D$); at $Re_D = 300$ mode B becomes dominant showing thin braids with spacing $\simeq D$ around the rollers.

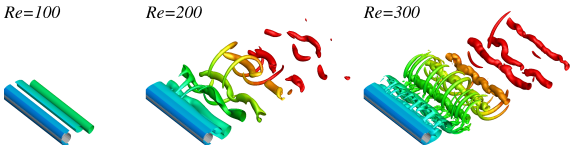

Figure 2: Q iso-surfaces in the wake of flow over cylinders.

The presence of the filaments on the lee side of the cylinder interferes with the instability process resulting in a topological change of the wake. The change in the wake shape also affects the value of the integral quantities such as the drag force. In particular, the filaments cause an elongation of the recirculation bubble that moves low-pressure region away from the lee side thus decreasing the drag. Figure 3 displays the shape of the recirculation regions with and without filaments. In general, a drag reduction between 4% to 10% and similar elongations are observed for all filaments with $l_f = D$ independent of their stiffness.

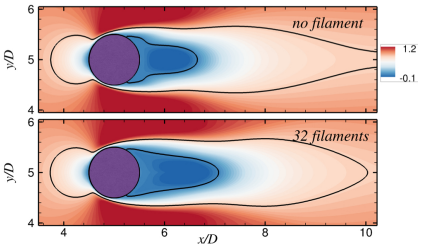

Figure 3: Contours of time-averaged u. Solid lines $u = 0.8$, and $u = 0$.

Differently, the instantaneous topology of the flow field strongly depends on the characteristics of filaments. Long and thin filaments with different but uniform spacings and various but constant flexibilities tend to inhibit higher order in modes in the wake. Figure 4 illustrates wake structures for three different flexibilities and two different spacings d_f. In all cases, braids and irregular fluctuations disappear. Softer filaments (smaller stiffness K_B) with $d_f = D$ cause larger footprints on the roller since they flap at greater amplitude. Note that d_f is a fraction of the mode A wavelength. While at much smaller d_f, flexibility does not play any role and filaments flap with a much smaller amplitude.

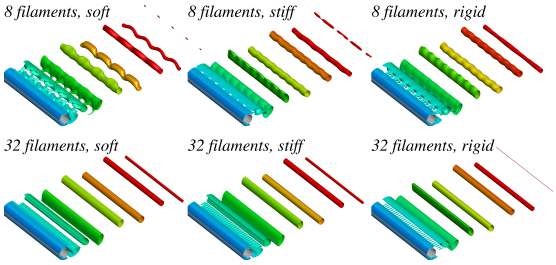

Figure 4: Q iso-surfaces at $Re = 200$ with filaments.

A further evidence of the effectiveness of the filaments in organising the wake structure is provided in Figure 5 showing the time spectrum of lift forces. Filaments narrow the energy content about a particular shedding frequency which is slightly greater than the shedding frequency at this Reynolds number. Smaller peaks in the figure correspond to super-harmonics of the shedding.

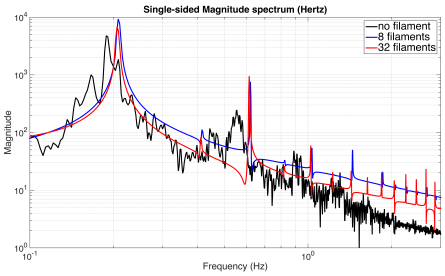

Figure 5: Spectrum of lift force at $Re_D = 200$.

At $Re_D = 300$, we compare the wake flow structures with different filaments spacings in Figure 6. For $d_f = D$, minimal changes occur in the wake, while for $d_f = D/4$ three-dimensionality of the wake almost disappears.

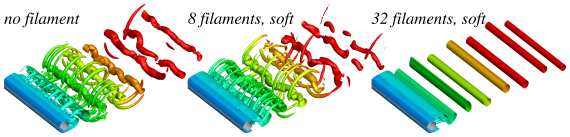

Figure 6: Q iso-surfaces at $Re = 300$ with and without filaments.

REFERENCES

[1] J. Favier, A. Revell, and A. Pinelli. A lattice boltzmann immersed boundary method to simulate the fluid interaction with moving and slender flexible objects. *J. Comput. Phys.*, 261:145–161, 2014.

[2] M. Omidyeganeh and U. Piomelli. Large-eddy simulation of two-dimensional dunes in a steady, unidirectional flow. *J. Turbul.*, 12(42):1–31, 2011.

[3] A. Pinelli, I.Z. Naqavi, U. Piomelli, and J. Favier. Immersed-boundary methods for general finite-difference and finite-volume Navier-Stokes solvers. *J. Comput. Phys.*, 229:9073—9091, 2010.

[4] C. H. K. Williamson. Vortex dynamics in the cylinder wake. *Annu. Rev. Fluid Mech.*, 28:477–539, 1996.